DOI: 10.1021/ma900896y

Macromolecules
ARTICLE

Modeling of Bottle-Brush Polymer Adsorption onto Mica and Silica Surfaces

Per Linse*,† and Per M. Claesson‡,§

†*Physical Chemistry, Center for Chemistry and Chemical Engineering, Lund University, Box 124, SE-221 00 Lund, Sweden,* ‡*Department of Chemistry, Surface and Corrosion Science, Royal Institute of Technology, SE-100 44 Stockholm, Sweden, and* §*Institute for Surface Chemistry, P.O. Box 5607, SE-114 86 Stockholm, Sweden*

Received April 24, 2009; Revised Manuscript Received June 16, 2009

ABSTRACT: The adsorption of a series of charged bottle-brush polymers with side chains of constant length on mica and silica surfaces is modeled using a lattice mean-field theory, and the predicted results are compared to corresponding experimental data. The bottle-brush polymers are modeled as being composed of two types of main-chain segments: charged segments and uncharged segments with an attached side chain. The composition variable X denotes the percentage of charged main-chain segments and ranges from $X = 0$ (uncharged bottle-brush polymer) to $X = 100$ (linear polyelectrolyte). The mica-like surface possesses a constant negative surface charge density and no special affinity, whereas the silica-like surface has a constant negative surface potential and a positive affinity for the side chains of the bottle-brush polymers. The model is able to reproduce a number of salient experimental features characterizing the adsorption of the bottle-brush polymers for the full range of the composition variable X on the two surfaces, and thereby quantifying the different nature of the two surfaces with respect to electrostatic properties and nonelectrostatic affinity for the polymer. In particular, the surface excess displays a maximum at $X \approx 50$ for the mica surface and at $X \approx 10$ for the silica surface. Moreover, the thickest adsorbed layer is obtained at $X = 10-25$.

Introduction

Bottle-brush polymers that consist of a linear backbone carrying a large number of covalently attached side chains have received great interest in recent years.[1,2] A large adsorption of such polymers with hydrophilic nonionic side chains has been shown to lead to low nonspecific protein adsorption,[3−6] strongly repulsive steric interactions,[7,8] and favorable lubrication properties,[9,10] with friction coefficients as low as achievable with efficient biochemical lubricants such as mucin.[11] A prerequisite for the successful use of physisorbed bottle-brush polymer layers in applications is a good understanding of their adsorption properties and how these are affected by the nature of the surface, the polymer architecture, solution composition, and interference by surfactants and other polymers present in solution. All these aspects have been investigated experimentally[7,10,12−17] using bottle-brush polymers synthesized from (i) poly(ethylene oxide) methyl ethyl methacrylate (PEO_{45}MEMA) and (ii) methacryloxyethlyl trimethylammonimum chlorid (METAC). The former monomer contains a 45 unit long oligo(ethylene oxide) chain and the latter a permanently charged cationic group. In the literature these polymers are referred to as PEO_{45}MEMA:METAC-X, where X stands for the mol % of charged segments.

It has been found that the adsorption of PEO_{45}MEMA:METAC-X polymers to silica surfaces is very sensitive to changes in pH and ionic strength, and this has been suggested to be primarily due to variations in the nonelectrostatic affinity between the PEO_{45} side chains and silica.[15−17] On the other hand, the adsorption to negatively charged mica surfaces has been suggested to be driven by only electrostatic interactions.[10] The surface excess and the number of surface attached PEO_{45} side chains as a function of polymer composition on these surfaces are shown in Figure 1.

We note large differences in the adsorption of PEO_{45}MEMA:METAC-X polymers on mica and silica. On mica, the low charge density bottle-brush polyelectrolytes ($X \leq 2$) do not adsorb, whereas maximum adsorption on silica is obtained in the composition range $0 < X < 10$. In contrast, on mica the maximum adsorption is achieved for $X = 50$. In this report, we provide further insight into the driving forces for adsorption of this type of bottle-brush polyelectrolytes onto mica-like and silica-like surfaces. In particular, we address: (i) the effects of polymer segment sequence, (ii) the influence of nonelectrostatic interactions, and (iii) the role of surface charge density. We approach the problem by using a self-consistent lattice mean-field theory to describe the adsorbed polymer layer, which provides detailed information on surface excess and polymer structure. The modeling approach allows a systematic variation of important parameters such as segment sequence, nonspecific surface affinity, and surface charge density that is not easily varied in experiments. Thus, we are able to draw important conclusions on how these properties affect adsorption and polymer layer structure.

Theoretical Model

The adsorption of bottle-brush polymers onto planar and negatively charged surfaces was modeled on the basis of a self-consistent-field theory, initially developed by Scheutjens and Fleer[18,19] and later extended to polyelectrolytes [see, e.g., ref 20 and references given therein] and branched polymers.[21] The extensions of electrostatic interactions and of branched polymers enter essentially independently into the theory, and hence bring no additional considerations. For the sake of briefness, we will here only give the main features of the theory; for more details we refer the reader to the original publications.

*Corresponding author.

 Published on Web 07/15/2009

Briefly, the space adjacent to a planar surface is divided into layers, and each layer is further divided into lattice cells of equal size. Within each layer the Bragg−Williams approximation of random mixing is applied, and thus all sites in a layer are equivalent. One lattice cell contains either (i) solvent, (ii) a polymer segment, (iii) a solvated cation, or (iv) a solvated anion. The polymer is composed of a main chain consisting of 200 segments of which (i) the percentage X is positively charged and (ii) the remaining percentage $100 - X$ is uncharged *and* has a side chain with 22 segments. In more detail, Figure 2a shows the structure of PEO_{45}MEMA and METAC used to synthesis the PEO_{45}MEMA:METAC-X bottle-brush polymer. In our coarse-graining, we represented (EO)MEMA with one uncharged segment, METAC with one charge segment, and $(EO)_2$ with one uncharged segment; hence, each chemical unit being of similar volume. Figure 2b illustrates the modeled bottle-brush polymer. The polymer is considered to be flexible, and the ordering of charged and uncharged segments of the main chain is random if nothing else is specified. When having a random sequence, for a given X the same random sequence is used, independent of other parameters. Polymers with the composition $X = 0$, 5, 10, 25, 50, 90, 95, and 100 are considered. The surface is modeled as having either a fixed surface charge density σ or a fixed surface potential ψ_s.

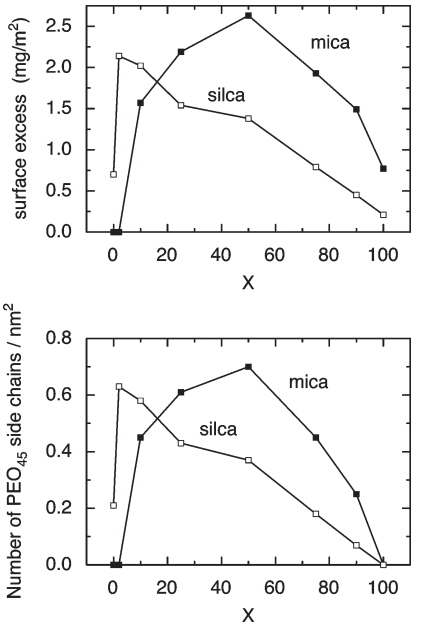

Figure 1. Experimental (a) surface excess and (b) adsorbed number of PEO side chains for adsorption of PEO_{45}MEMA:METAC-X on mica (filled symbols) and silica (open symbols) surfaces at pH = 5.5−6 and ionic strength ≤0.1 mM. Data taken from refs 7 and 15.

There are two different types of interactions in the model: electrostatic (charge−charge) and nonelectrostatic (the rest). The nonelectrostatic interaction between species in adjacent lattice sites is described by Flory−Huggins χ-parameters.[22] The same description is used for the interaction with the surface. Since only the differences of the interaction parameters involving a surface are relevant, we introduce $\Delta\chi_\alpha = \chi_{\alpha,\text{surface}} - \chi_{\text{solvent,surface}}$, α being a main-chain or a side-chain segment. The relation to the adsorption parameter χ_s is given, e.g., for the polymer by $\chi_s = -\lambda_{1,0}\Delta\chi_{\text{polymer}}$, $\lambda_{1,0}$ being the fraction of all neighbors of a site in layer 1, which resides in the surface layer. Here, $\lambda_{1,0} = {}^1/_4$, since a hexagonal lattice was selected. The lattice topology only affects the λ matrix, and the outcome of the results is only mildly affected by the choice of lattice topology.

In line with the random mixing approximation, charged species (charged polymer segments and salt species) are assumed to interact with a potential of mean force, ψ_i, which depends only on the distance to the surface (layer number i). The potential of mean force is related to the charge density through Poisson′s equation, $-\varepsilon_0\varepsilon_r\nabla^2\psi_i = \rho_i$, where $\varepsilon_0\varepsilon_r$ is the dielectric permittivity of the medium and ρ_i is the total charge density in layer i. The charges of the species are located to planes in the middle of each lattice layer, and the space in between the charged planes is free of charge. A uniform dielectric permittivity is used.

From the set of volume fraction profiles of the species, $\{\phi_{Ai}\}$, and the interaction parameters, a nonelectrostatic potential u_{Ai} can be calculated for species A in layer i. There is also a layer dependent but species independent hard-core potential, u'_i, acting on each species. This potential is essentially the lateral pressure and is responsible for making the volume fraction in each layer sum up to one. Given the nonelectrostatic potential u_{Ai} and the electrostatic energy $q_A\psi_i$ of species A in layer i as well as the hard

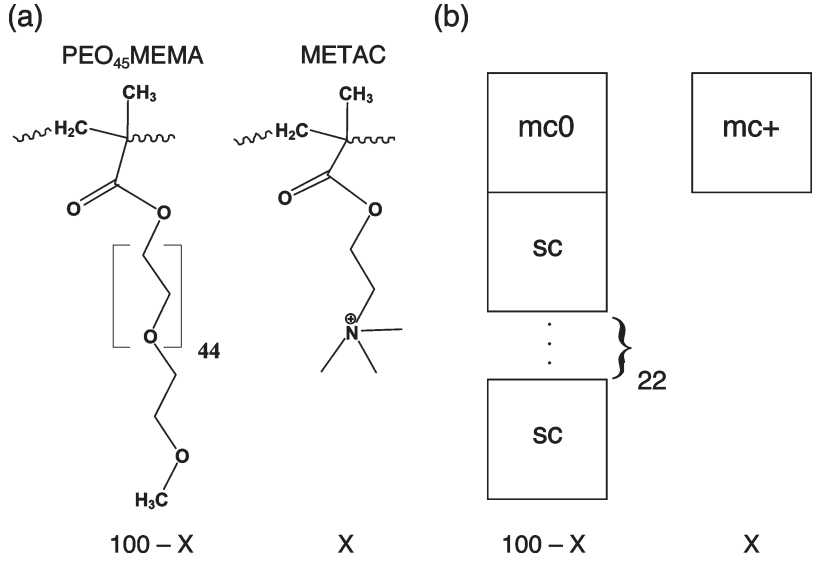

Figure 2. (a) Molecular structures of (left) PEO_{45}MEMA and (right) METAC units of the bottle-brush polymer PEO_{45}MEMA:METAC-X and (b) the coarse-grained model of the two units, (left) the first one composed a uncharged main-chain segment (mc0) and 22 uncharged side-chain segments (sc) and (right) the second one of a positively charged main-chain segment (mc+). X denotes the fraction of METAC units and consequently also the fraction of charged main-chain segments in the copolymer.

Table 1. Model Parameters

quantity	value
temperature	$T = 298$ K
relative dielectric permittivity	$\varepsilon_r = 80$
lattice spacing	$d = 0.5$ nm
degree of polymerization (main chain)	$r_{\text{main-chain}} = 200$
degree of polymerization (side-chain)	$r_{\text{side-chain}} = 22$
bulk polymer volume fraction	$\phi_{\text{polymer}} = 1 \cdot 10^{-4}$
bulk salt volume fraction	$\phi_+ = \phi_- = 3 \cdot 10^{-4}$
surface charge density[a]	$\sigma = -0.2$ (mica-like surface)
surface potential	$\psi_s = -0.1$ V (silica-like surface)
interaction parameters[b]	$RT\chi_{\text{side-chain,water}} = 1.3$ kJ/mol
	$RT\Delta\chi_{\text{side-chain}} = 0$ kJ/mol (mica-like surface)
	$RT\Delta'\chi_{\text{side-chain}} = -10$ kJ/mol (silica-like surface)
conversion factors[c]	$C_{\text{salt}}/\text{M} = 13.3\phi_{\text{salt}}$

[a] Number of elementary charges per d^2. [b] Other interaction parameters are zero. [c] Obtained from the size of a lattice cell.

core potential u'_i of layer i, the distribution of *unconnected* segments of type A is given by the Boltzmann weight of the sum of the three terms, $\phi_{Ai} \sim \exp[-(u_{Ai} + u'_i + q_A\psi_i)/kT]$. For polymers, the matter becomes more complex since the connectivity has to be taken into account. Finally, since $\{\phi_{Ai}\}$ depends on $\{u_{Ai}\}$ and $\{\psi_i\}$, and $\{u_{Ai}\}$ and $\{\psi_i\}$ are functions of $\{\phi_{Ai}\}$ as indicated above, $\{\phi_{Ai}\}$, $\{u_{Ai}\}$, and $\{\psi_i\}$ have to be solved self-consistently. A numerical solution of this set of implicit and nonlinear equations was carried out using up to 100 layers.

Parameters used in the model calculations of the adsorption of the bottle-brush polymers onto mica-like and silica-like surfaces are compiled in Table 1. Some of the parameters (T, ε_r, X, r_{polymer}, ϕ_{polymer}, and ϕ_{salt}) are known characteristics of the experimental systems. The values of some other parameters (d, σ, and ψ_s) are less obvious and some reasonable assignments were used. Here, we have adopted the lattice cell length $d = 0.5$ nm and, furthermore, $\sigma = -0.2$ (thus constant surface charge density) for the mica-like surface and $\psi_s = -0.1$ V (thus constant surface potential) for the silica-like surface at pH = 6. Noticeable is that the combination of d and ϕ_{salt} gives formally a salt concentration 40 times larger than the typical experimental one in our comparison. Unfortunately, no numerical solution was found at substantially lower ϕ_{salt} in some parts of the parameter subspace with $\sigma = -0.2$. Finally, we have the remaining parameters: $\chi_{\text{main-chain,solvent}}$, $\chi_{\text{side-chain,solvent}}$, $\Delta\chi_{\text{main-chain}}$, and $\Delta\chi_{\text{side-chain}}$. First, for simplicity, we assigned $\chi_{\text{main-chain,solvent}} = \Delta\chi_{\text{main-chain}} = 0$, since for low X the number of side chains grossly exceeds the number of main chains and hence the interaction involving the side chains is more important, and at high X the electrostatics dominates. Furthermore, we adopted $RT\chi_{\text{side-chain,solvent}} = 1.3$ kJ/mol as being a reasonable value for the EO−water interaction.[23] Finally, we used $RT\Delta\chi_{\text{side-chain}} = 0$ for describing the EO−mica interaction and $RT\Delta\chi_{\text{side-chain}} = -10$ kJ/mol (fitted) for the EO−silica interaction at pH = 6. Experimentally it is known that uncharged PEO brush polymers does not adsorb onto mica,[7] whereas it strongly adsorbs onto silica at pH = 6.[15]

On the basis of the volume fraction profiles $\{\phi_{Ai}\}$, the adsorbed amount of species A expressed as the surface excess of species A is evaluated according to $\Gamma_{\text{exe,A}} = \Sigma_i(\phi_{Ai} - \phi_{A,\text{bulk}})$, where the summation extends over all lattice layers. The polymer surface excess is given by $\Gamma_{\text{exe}} = \Gamma_{\text{exe, main-chain}} + \Gamma_{\text{exe, side-chain}}$.

Results

We will first present results obtained from modeling the adsorption onto the mica-like and silica-like surfaces and discuss those with respect to experimental findings. Thereafter, we will examine three aspects more thoroughly, viz. how (i) polymer segment sequence, (ii) nonelectrostatic polymer−surface affinity, and (iii) electrostatic interactions affect the adsorption.

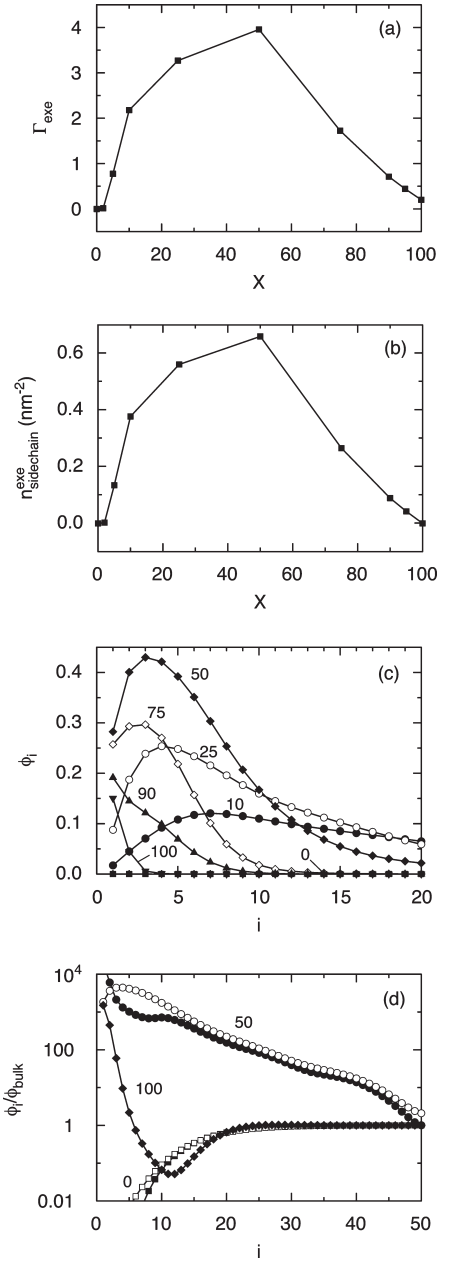

Figure 3. Theoretical adsorption at the mica-like surface displaying (a) surface excess Γ_{exe} as a function of the composition X, (b) excess adsorbed number of side chains as a function of the composition X, (c) polymer segment volume fraction ϕ_i as function of layer number i at composition $X = 0$ (filled squares), $X = 10$ (filled circles), $X = 25$ (open circles), $X = 50$ (filled diamonds), $X = 75$ (open diamonds), $X = 90$ (filled triangles), and $X = 100$ (filled nablas), and (d) species volume fraction profiles divided by corresponding bulk volume fraction ϕ/ϕ_{bulk} as function of layer number i for main-chain (solid symbols) and side-chain (open symbols) segments at $X = 0$ (squares), $X = 50$ (circles), and $X = 100$ (diamonds). Parameters as given in Table 1.

Mica-Like Surface. The mica-like surface is characterized as a highly charged surface of constant surface charge density, oppositely charged to that of the bottle-brush polyelectrolyte, and with no nonelectrostatic affinity for main-chain and side-chain segments.

Figure 3a shows the calculated surface excess Γ_{exe} as a function of the bottle-brush composition X on the mica-like

surface. We note that uncharged and very low charged ($X \leq 2$) bottle-brush polymers do not adsorb onto the mica-like surface, which is due to the lack of affinity for the surface. The surface excess Γ_{exe} increases with increasing charge density of the bottle-brush polymer up to $X = 50$. At even higher X, the surface excess decreases. Qualitatively, this is in excellent agreement with the experimental findings[7] illustrated in Figure 1a. In particular, both modeling and experiments show no adsorption for low charge density bottle-brush polyelectrolytes ($X \leq 2$) and an adsorption maximum at $X = 50$. A small discrepancy between the modeling and the experimental results is that the curvature of Γ_{exe} vs X for $X > 50$ is different; experimentally the shape is convex but slightly concave for the modeling results.

The predicted surface excess expressed as the number of side chains per unit area is given in Figure 3b. The appearance is similar to that for the surface excess Γ_{exe} shown in Figure 3a. An obvious difference appears for $X = 100$, where the number of side chains at the surface is zero due to the absence of such side chains in the polymer, whereas the adsorbed mass is nonzero. Again, both experiments and modeling show a maximum for $X = 50$, and at this composition the number of side chains of adsorbed polymers in both cases slightly exceeds 0.6 nm^{-2} (see Figures 1b and 3b). This result demonstrates that our choice of parameters, in particular the lattice size d, is reasonable.

Calculated polymer segment density profiles for different polymer compositions are given in Figure 3c. For $X \leq 75$ we note a maximum in the polymer segment volume fraction away from the surface, and the maximum moves to larger distances as the charge density of the bottle-brush polyelectrolyte is decreased. This is a consequence of (i) the overall lower electrostatic affinity for the surface by the main chain and (ii) the increased number of side chains that are repelled from the surface. The modeling results also show that the polymer layer is most extended in the composition range $10 \leq X \leq 25$. There are no neutron reflectivity data that we can compare our results with, but we can make a qualitative comparison with the force data reported by Naderi et al.[7] They note that the most long-range steric forces were observed for $X = 10$, in agreement with the model calculations. However, the measured force profiles indicate a less extended layer for $X = 25$, which is not consistent with the modeling results. Experiments demonstrate that the strongest steric repulsion is achieved for $X = 50$, consistent with the highest segment density found for this polymer composition by modeling. Experiments and modeling do also agree in the conclusion that the polyelectrolyte without side chains ($X = 100$) adsorbs in a very flat conformation and that addition of a relatively small number of side chains ($X = 75-90$) results in a compact and relatively thin adsorbed polymer layer.

Figure 3d shows selected segment density profiles normalized by the corresponding segment density in bulk (far from the surface). This quantity will be referred to as the accumulation factor. It is seen that the uncharged bottle-brush polymer ($X = 0$) is depleted from the surface region, which is a consequence of the entropic penalty of confining the polymer to the solution next to the surface. On the other end of the scale, the linear polyelectrolyte ($X = 100$) is strongly accumulated with a segment density that decreases rapidly away from the surface. This is a consequence of the strong electrostatic polyelectrolyte−surface affinity, involving an entropy gain from the release of surface and polyelctrolyte counterions occurring upon polyelectrolyte adsorption. We also note a weak depletion in the distance region $6 \leq i \leq 25$, after which the bulk concentration of segments is obtained. This demonstrates that adsorption of the linear polyelectrolyte results in a small charge reversal, in agreement with experiments.[7] For the 50% charged bottle-brush polyelectrolyte ($X = 50$) the main-chain segments are more strongly accumulated at the surface than the side-chain segments, but this reverses further away from the surface ($i \geq 3$).

Silica-Like Surface. The silica-like surface is also oppositely charged to the bottle-brush polyelectrolyte, but possesses a constant surface potential to capture effects originating from the charge regulating ability of the silanol groups. The magnitude of the resulting charge density is always lower than that of the mica-like surface. The side-chain segments, but not the main-chain segments, have a nonelectrostatic affinity to the surface, which is another important difference to the mica-like surface discussed above.

The calculated surface excess Γ_{exe} on the silica-like surface as a function of the bottle-brush composition X is given in Figure 4a (solid symbols), whereas the corresponding experimental data on silica are shown in Figure 1a. The adsorption of the uncharged bottle-brush polyelectrolyte ($X = 0$) on the silica-like surface is large, whereas no adsorption was found on the mica-like surface. This is a consequence of the nonelectrostatic affinity between the side-chain segments and the surface and in agreement with experimental results. Introduction of a small number of charged segments increases the adsorption on the silica-like surface, and the maximal Γ_{exe} is found for $X = 10$, which is significantly lower than that on the mica-like surface. This is also due to the side-chain affinity to the silica-like surface. At higher X, the surface excess decreases. Experimentally, the maximal adsorption is observed at somewhat lower bottle-brush charge densities ($X = 2$), and introduction of a small amount of charges on the main chain has a more dramatic effect on Γ_{exe} than predicted by the modeling. Possible reasons for these discrepancies between experiments and modeling results will be discussed below.

Figure 4a (open symbols) also shows the surface excess for a silica-like surface with the constant surface charge density $\sigma = -0.02841$; σ selected such that $\psi_s = -0.1$ V is obtained for a polymer solution at $X = 0$. For low charged bottle-brush polyelectrolytes, very similar results are obtained under constant σ and constant ψ_s conditions. On the other hand, for larger X, the charge regulating ability of the surface is important, and larger Γ_{exe} is found on the constant ψ_s-surface than on the constant σ-surface. The results obtained for the constant ψ_s silica-like surface agree better with experimental data than those obtained by assuming a constant σ. Thus, below we consider the constant ψ_s-surface, if not otherwise stated.

The number of side chains per unit area on the silica-like surface is shown in Figure 4b, and these results can be compared with the experimental data in Figure 1b. For high bottle-brush charge densities ($X \geq 20$), a quantitative comparison between the data in Figures 1b and 4b show a good agreement, again validating the choice of the lattice size. We note that it is a nontrivial result that this is the case for both the mica-like and silica-like surfaces.

Polymer segment density profiles for the adsorbed layers on the silica-like surface are given in Figure 4c. A notable difference compared to the mica-like surface is that in all cases the polymer segment density is highest at the surface. This is a consequence of the nonelectrostatic affinity between the side chains and the surface. The most extended polymer layer is found in the composition range $5 \leq X \leq 25$, which is qualitatively in agreement with the conclusions drawn from combined analysis of QCM-D and reflectometry data.[15,17]

The accumulation factors depicted in Figure 4d show that both main-chain and side-chain segments are strongly

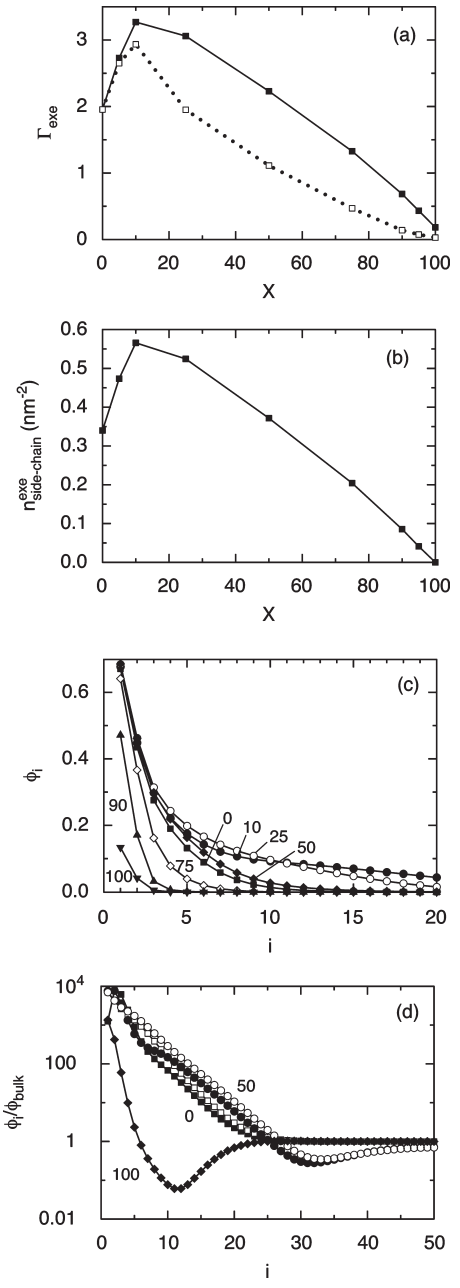

Figure 4. Theoretical adsorption at the silica-like surface displaying (a) surface excess Γ_{exe} as a function of the composition X (solid symbols), (b) excess adsorbed number of side chains as a function of the composition X, (c) polymer segment volume fraction ϕ_i as function of layer number i at composition $X = 0$ (filled squares), $X = 10$ (filled circles), $X = 25$ (open circles), $X = 50$ (filled diamonds), $X = 75$ (open diamonds), $X = 90$ (filled triangles), and $X = 100$ (filled nablas), and (d) species volume fraction profiles divided by corresponding bulk volume fraction ϕ_i/ϕ_{bulk} as function of layer number i for main-chain (solid symbols) and side-chain (open symbols) segments at $X = 0$ (squares), $X = 50$ (circles), and $X = 100$ (diamonds). Parameters as given in Table 1. In part a, corresponding data but for a surface with the constant surface charge density $\sigma = -0.02841$ are also given (open symbols).

accumulated next to the surface. For the uncharged bottle-brush, the side-chain segments are more strongly accumulated at the surface ($\phi_1/\phi_{bulk} \approx 10^4$) than the main-chain segments ($\phi_1/\phi_{bulk} \approx 10^3$), which is due to the nonelectrostatic affinity of the side chains for the surface. For $X = 50$, main-chain and side-chain segments are accumulated to similar extent in the surface layer, but the main-chain segments

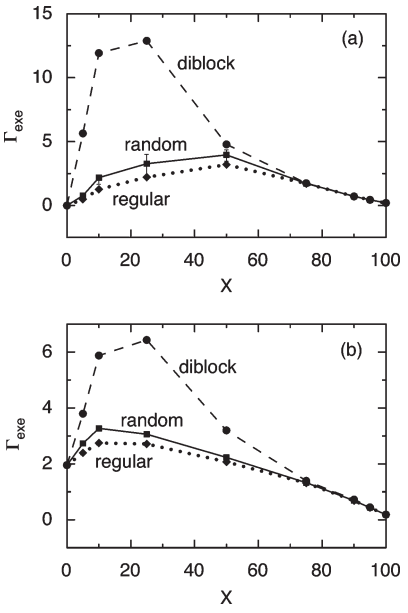

Figure 5. Theoretical surface excess Γ_{exe} as a function of the composition X for the (a) mica-like and (b) silica-like surfaces with random (squares), regular (dimonds), and diblock (circles) distributions of the uncharged and charged main-chain segments. Other parameters as given in Table 1. In part a, the fluctuations of Γ_{exe} given as twice the standard deviation for 100 realizations of random distributions are also given as error bars.

dominate in layers 2 and 3, whereas the side-chain segments are more strongly accumulated further out in the adsorbed polymer layer. Finally, also on silica-like surfaces a charge reversion occurs for the highly charged polyelectrolytes, as evidenced by the development of a depletion region.

Effects of Polymer Segment Sequence. The bottle-brush polyelectrolytes used in the experiments that we compare our modeling results with were prepared by free-radical polymerization.[16] This method results in a large length polydispersity and, owing to different reaction rates of the monomers, also in a composition polydispersity. It has previously been shown for uncharged diblock copolymers that such composition polydispersity may have a large effect on the adsorption behavior.[24] This motivates a theoretical investigation of the importance of the polymer segment sequence on the adsorption properties of bottle-brush polylectrolytes. To this end we, in addition to the random distribution of charged and uncharged main-chain segments used for calculating the results given in Figures 3 and 4, also considered (i) a completely regular distribution of these segments and (ii) a complete separation of these segments into one charged block and one uncharged block.

Figure 5 shows the effect of the sequence of the segments in the bottle-brush polyelectrolytes and the fluctuations of Γ_{exe} for a set of random distributions for adsorption on the mica-like and silica-like surfaces. For high charge density bottle-brush polyelectrolytes ($X \geq 75$) the exact sequence of the charged groups and the uncharged groups with long side chains play a minor role for the adsorption on both mica-like (Figure 5a) and silica-like (Figure 5b) surfaces. For bottle-brush polyelectrolytes with lower charge densities, the sequence plays a role but the difference in the surface excess between the random and regular sequences is rather small, with a slightly higher Γ_{exe} obtained for the random sequence. The differences are approximately twice the standard deviation of the fluctuations of Γ_{exe} for the random distribution. This demonstrates that some blockiness favors adsorption,

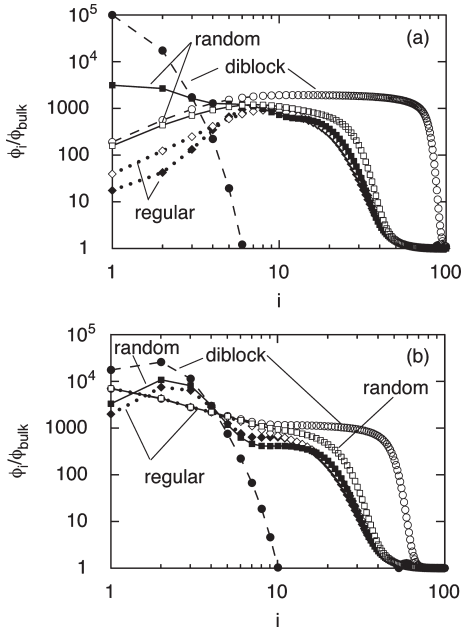

Figure 6. Theoretical volume fraction of uncharged (open symbols) and charged (filled symbols) main-chain segments divided by their corresponding bulk volume fraction $\phi_i/\phi_{i,bulk}$ as function of layer number i for (a) mica-like and (b) silica-like surfaces with random (squares), regular (diamonds), and diblock (circles) distribution at the composition $X = 10$. Note the logarithm scale of the abscissa. Other parameters as given in Table 1.

as also observed for linear polyelectrolytes.[20] The extreme case of blockiness corresponds to a diblock copolymer consisting of one charged block and one uncharged block with grafted side chains. Clearly, when the fraction of charged main-chain segments is low ($X < 50$ but larger than zero) such a segment distribution results in a much higher Γ_{exe} than obtained for the random and regular segment distributions. Finally, the surface excesses obtained for the random sequences selected for the different X fall within two standard deviation of the distribution of Γ_{exe} evaluated using 100 different random sequences (Figure 5a). Hence, the random sequences used for the different X are representative.

Experimentally, it was found that addition of a small amount of charged segments ($2 \le X \le 10$) to the uncharged bottle-brush resulted in a 3-folded increase in surface excess (Figure 1a), whereas modeling results using a random segment distribution indicated an increase only by a factor of 1.5 (Figure 4a). Our calculations show that in principle this could be explained by a blockiness of the low charge density bottle-brush polyelectrolyte (Figure 5b). However, if this indeed was the case, then the effect should be similar on the mica-like surface (Figure 5a), but experiments (Figure 1a) show that this is not the case. Thus, considering all these results together: (i) we conclude that the real polymers used in the experiments do not have a blockiness that significantly exceeds that expected for a random distribution, and (ii) we have to look for other reasons for why modeling and experiments do not agree for low charge density bottle-brush polymers on the silica-like surface.

The effects of the segment sequence on the polymer layer for the mica-like and silica-like surfaces for the 10% charged polymer ($X = 10$) are given in Figure 6. The regular polymer architecture (dotted curves) displays a rather small segregation of main-chain and side-chain segments on both mica-like and silica-like surfaces. At the other end of the spectrum, the diblock polymer (dashed curves) shows large segregation of main-chain and side-chain segments, with the former being accumulated close to the surface and the latter extending away from the surface. Due to the lack of nonelectrostatic affinity between the side chains and the mica-like surface, the segregation is more pronounced on this surface than on the silica-like surface. The random-segment distribution (squares) falls in between these two extremes. For this polymer architecture, the segregation is pronounced on the mica-like surface with a large accumulation of main-chain segments close to surface and a higher accumulation factor of side-chain segments away from the surface ($i > 5$). In contrast, the segregation is significantly smaller at the silica-like surface due to the nonelectrostatic side-chain affinity to this surface. In fact, the accumulation factor is larger for the side-chain segments in layer 1, the main-chain segments are more strongly accumulated in layers 2−4, and further away from the surface the side-chain segments are again most strongly accumulated.

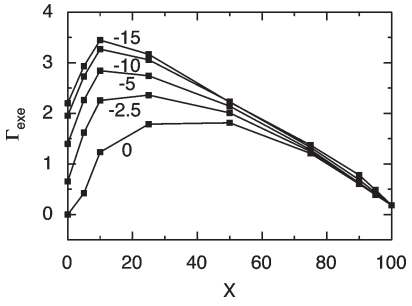

Figure 7. Theoretical surface excess Γ_{exe} as a function of the composition X for the silica-like surface at indicated values of $RT\Delta\chi_{side\text{-}chain}$. Other parameters as given in Table 1.

Effect of Nonelectrostatic Side-Chain Surface Affinity. The nonelectrostatic surface affinity of the side chains is expected to play a crucial role for the adsorption of the bottle-brush polyelectrolytes as seen by comparing the data reported in Figures 3 and 4. It is also known that the adsorption of poly(ethylene oxide) and poly(ethylene oxide) containing polymers onto silica decreases strongly with increasing pH and ionic strength,[25,26] a feature that can be explained by a decreased nonelectrostatic affinity with increasing surface charge density of the silica surface. It is thus of interest to investigate how a change in side-chain affinity will affect the adsorption of bottle-brush polyelectrolytes.

Figure 7 displays the surface excess Γ_{exe} as a function of the composition X for the silica-like surface, but at different values of the side-chain−surface affinity. If the side-chain affinity to the surface is zero, then a mica-like behavior is recovered, with no adsorption of the uncharged bottle-brush ($X = 0$) and a maximum near $X = 50$. The adsorption in the low charge density regime ($X < 50$) increases substantially with increasing side-chain affinity until this parameter, $RT\Delta\chi_{side\text{-}chain}$, reaches a value of about −10. A further increase in side-chain affinity hardly has any effect since the surface layer is close to saturated with side-chain segments. Thus, our modeling results demonstrate that Γ_{exe} of low charge density bottle-brush polymers depend crucially on the side-chain affinity. Furthermore, our findings are consistent with the experimental observation[15,16] that the strong pH and ionic strength dependence for the adsorption of bottle-brush polymers with PEO side chains on silica could be explained by changes in nonelectrostatic affinity of the side chains toward the surface. On the other hand, Γ_{exe} of the high charge density bottle-brush polymers ($X \ge 50$) is only weakly affected by the nonelectrostatic surface affinity. This finding is rationalized by the predominance of electrostatic interactions, which results

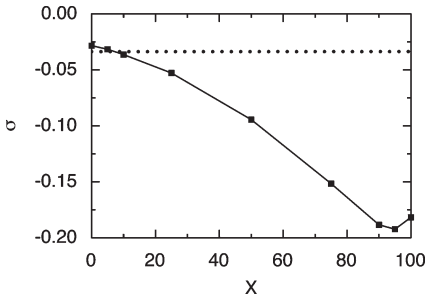

Figure 8. Theoretical surface charge density σ for the silica-like surface as a function of the composition X (solid curve) and corresponding surface charge density for a polymer-free salt solution (dotted line). Other parameters as given in Table 1.

in a high density of charged main-chain segments at the surface.

Electrostatic Effects. We have already shown in Figure 4a that the charge regulating ability of the silica-like surface is important for the surface excess of the bottle-brush polyelectrolytes. This aspect is further analyzed in Figure 8. As a reference, the charge density of the silica-like surface in polymer-free salt solution is used (dotted line). Adsorption of the uncharged bottle-brush polymer ($X = 0$) results in a small reduction of the magnitude of the surface charge density $|\sigma|$. This is due to a partial exclusion of surface counterions from the surface region by the volume of the adsorbed polymers. Such a reduction of the counterion concentration next to a charged surface is electrostatically unfavorable and a surface with titrable groups responds by reducing $|\sigma|$.

When the bottle-brush polyelectrolyte charge density is increased by addition of a few percentage of charged groups, the lowering of $|\sigma|$ is reduced, until $X = 7$, where no change in σ occurs due to the adsorption of the polymer. At even larger bottle-brush polyelectrolyte charge density, $|\sigma|$ increases due to polymer adsorption, and more so for the more highly charged polyelectrolytes. We note that the maximal $|\sigma|$ is achieved for $X = 95$ and not for $X = 100$, which is caused by the nonelectrostatic affinity between the surface and the side chains that brings some additional charged segments in the close vicinity of the silica surface. Finally, the assumption of a constant surface potential ψ_s implies an infinite number of charge regulating sites. This is obviously not correct; on a real silica surface the number of silanol groups is limited. A value of 4−5 silanol groups nm^{-2} has been suggested by Zhuravlev,[27] but this value will depend on the surface treatment of the silica substrate. As a result, the effect discussed above will occur on a real silica surface, but the magnitude of the variation of the surface charge density could be lower. Nevertheless, the silanol density given above implies the hypothetical $|\sigma|_{max} \approx 1$, which is larger than $|\sigma| = 0.19$ as being the largest value obtained at $X = 95$.

To shed some further light on the role of electrostatic interactions on the adsorption of bottle-brush polyelectrolytes onto the mica-like and silica-like surfaces, we have also examined the adsorption of analog systems but without electrostatic interactions (below referred to as uncharged systems). Beside the original surface excess Γ_{exe} of the charged systems (solid curves), Figure 9 also displays corresponding Γ_{exe} of the uncharged systems (dotted curves) and Γ_{exe} corresponding to the charge equivalence of the surface charge (dashed curves).

On the mica-like surface there is a weak depletion for all side-chain densities of the uncharged system (Figure 9a). This is an obvious result since there is neither electrostatic nor nonelectrostatic driving force for the adsorption. For the charged case at $X \geq 75$, the charges of the polyelectrolyte closely balances (but slightly overcompensates) the surface charges and the adsorption limit is set by the electrostatics. At lower bottle-brush charge densities, the charges of the mica-like surface is not compensated by the charges of the adsorbed polyelectrolytes. Hence, in this case adsorption is limited by excluded-volume effects from (mainly) side-chain segments. These conclusions are consistent with experimental results.[7]

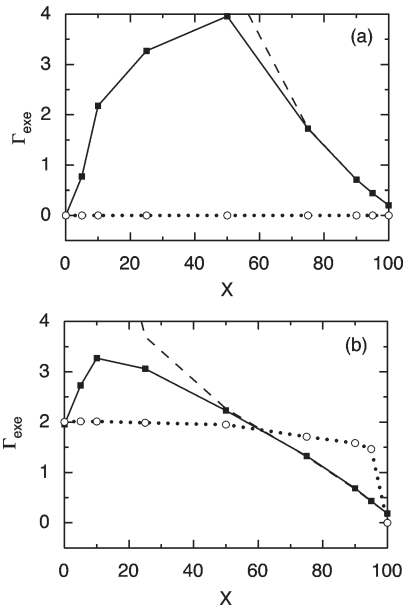

Figure 9. Theoretical surface excess Γ_{exe} (solid curves) and corresponding data without electrostatic interaction (dotted curves) as a function of the composition X for the (a) mica-like and (b) silica-like surfaces. Other parameters as given in Table 1. The surface excess corresponding to charge equivalence is also shown (dashed curves).

For the silica-like surface a different picture emerges (Figure 9b). Due to the high nonelectrostatic affinity between the surface and the side chains, high Γ_{exe} is achieved for the uncharged system with a bottle-brush polymer containing 1 side chain per 1 main-chain segment down to 1 side chain per 20 main-chain segments ($0 \leq X \leq 95$). The independence of Γ_{exe} on polymer architecture in this region is due to that the adsorption proceeds until the surface is close to fully covered by side-chain segments (see Figure 4c). Only for even less side chains on the polymer does a sharp reduction in surface excess occur. By comparing Γ_{exe} of the charged system with the uncharged one, it can be concluded that for large charge densities ($X > 60$) Γ_{exe} of the charged system is lower than that of the uncharged one. Thus, electrostatics limits the adsorption that occurs to close to charge neutrality. For the less charged bottle-brush polymers, adsorption does not proceed to charge neutrality but is limited by excluded-volume effects. In this region the electrostatic affinity increases the adsorption of the charged bottle-brush polymers.

Similar analysis has been made for the silica-like surface but at constant surface charge density (data not shown). Most noticeable is a more extended interval ($25 \leq X < 100$) of overcharging, and the relative overcharging amounts to a factor of 2 at $X \approx 60$.

Discussion and Conclusions

On the basis of mean-field lattice calculations, the adsorption of charged bottle-brush polymers of various compositions onto

two different oppositely charged and planar surfaces mimicking mica and silica have been investigated. Realistic parameters have been assigned, whenever possible. To obtain modeling results corresponding to experimental data, the mica surface was represented by a surface with a high constant surface charge density, whereas the silica surface was modeled as a surface with constant surface potential. Furthermore, the polymer−mica interaction was athermal, whereas an attractive side-chain−surface interaction was assigned for the silica surface. Thus, the two surfaces differed in two important aspects.

Despite the limitations of the present model and experimental uncertainties in length and composition polydispersity, we obtained a surprisingly good representation of the surface excess and the number of adsorbed side chains per surface area as a function of polymer architecture, spanning the composition range from $X = 0$ corresponding to an uncharged bottle-brush polymer to $X = 100$ corresponding to a linear polyelectrolyte. As to the mica-like surface, the surface excess is a balance of the attractive electrostatic polymer−surface interaction, the repulsive electrostatic polymer−polymer interaction, and the repulsive conformational entropy change due to adsorption. Linear polyelectrolytes often display a maximal surface excess at $X \approx 1-5$[28−30] (in the present notation); hence, the presence of the repulsive contribution of the side chains shifts the optimal X to higher linear charge density (here $X = 50$). For the adsorption onto the silica-like surface, the effect of the nonelectrostatic attractive side-chain−surface interaction becomes larger at decreasing X, and this attraction restores the appearance of the maximal surface excess to a low value of X.

We have also used the mean-field lattice model to investigate the effect of polymer segment sequence, side-chain−surface affinity, and the role of the electrostatic interactions *separately*—a task rarely feasible experimentally. We observed that the difference in surface excess between regular and random distributions is at most 20%, whereas over a 5-fold difference in excess amount between regular and diblock distributions was obtained. The largest difference was obtained in the polymer composition interval $10 \leq X \leq 30$.

The strongly increasing surface excess with X for $X \leq 10$ suggests that composition polydispersity in combination with blockiness may be an important consideration in modeling the surface excess. The discrepancy in the location of the maximal surface excess between experiments and modeling results for silica could possibly be explained by this. However, the very consistence of modeling and experiments for the mica surface with the same polymers makes this explanation less likely.

Another discrepancy between modeling results and experiments is the larger predicted excess amount at $X = 0$ for the silica-like surface and the more dramatic effect on introduction of a small amount of charges in the polymer structure observed experimentally compared to modeling, cf. Figures 1b and 4a. A variation in side-chain−surface affinity does not provide any better fit to the experimental data, see Figure 7. A possible explanation is that the assumption of a flexible chain made in the model is too simplified. SAXS and SANS experiments have shown that the bottle-brush polymers in solution adopt rod-like conformations with a Kuhn-length in the order of 20−30 nm,[16,31] which is due to excluded-volume repulsion between the side chains. Viscoelastic modeling of QCM-D data on the adsorption of bottle-brush polymers on silica has shown that the uncharged bottle-brush adopts a flat conformation on the surface.[17] Introduction of a small amount of charges in the polymer architecture results in an intricate adsorption process, where the polymer first adsorbs in a flat conformation, but as the adsorption proceeds a clear structural transition into a more extended conformation occurs, presumably resulting from accumulation of charged segments next to the surface that forces the uncharged regions to extend into solution.[17] We speculate that the intrinsic stiffness of the chain, and the associated bending energy, is responsible for these features, and that our modeling approach does not capture this effect fully.

It is experimentally known that the EO−silica interaction depends on the degree of deprotonation of the silanols group on the silica surface—it becomes less attractive as silica is deprotonated.[15,25,26] Therefore, assigning a constant EO−silica surface interaction parameter is expected to be an approximation in cases as here, where the silica surface charge density is varying. The increased magnitude of the surface charge density (Figure 8) suggests that the EO−silica surface interaction parameter should be less negative at increasing X. It also shows that an increase in pH and ionic strength, that increases the surface charge density of silica and reduces the side-chain−surface affinity, will result in a more mica-like behavior, as quantified in Figure 7. This is also observed experimentally.[15] In a recent work, Postmus et al.[32] have performed similar lattice mean-field modeling of the adsorption of PEO on silica surfaces. In their more elaborated model, they have, in particular, included silica surface charge titration and polymer−surface interaction parameters that depended on the surface deprotonation, which lead to a reduced PEO adsorption at increasing pH and salt concentration in accordance with experiments.

From comparison with the analogous uncharged systems, we conclude that the adsorption of the bottle-brush polymers is driven by the electrostatic polymer−surface interaction at $X > 0$ for the mica-like surface, and in the interval $0 < X \leq 60$ for the silica-like surface, whereas at $X > 60$ for the silica-like surface the electrostatic repulsion between the adsorbed polymer chains limits the adsorption.

After the construction of a model capable to reproduce a number of experimental features concerning the adsorption of random bottle-brush copolymers with variable main-chain composition on two different surfaces, it would be interesting to expand the use of the model. In particular, it would be of value to confront (i) predicted adsorption of bottle-brush polymers with a diblock main-chain architecture, as given here, and (ii) predicted adsorption of bottle-brush polymers with variable side-chain length with experimental data.

Acknowledgment. P.L. and P.M.C. acknowledge financial support from the Swedish Research Council (VR).

References and Notes

(1) Zhang, M.; Muller, A. H. E. *J. Polym. Sci., Part A: Polym. Chem.* **2005**, *43*, 3461–3481.
(2) Gorochovceva, N.; Naderi, A.; Dedinaite, A.; Makuska, R. *Eur. Polym. J.* **2005**, *41*, 2653–2662.
(3) Huang, N.-P.; Michel, R.; Voros, J.; Textor, M.; Hofer, R.; Rossi, A.; Elbert, D.; Hubbell, J. A.; Spencer, N. D. *Langmuir* **2001**, *17*, 489–498.
(4) Zhou, Y.; Liedberg, B.; Gorochovceva, N.; Makuska, R.; Dedinaite, A.; Claesson, P. M. *J. Colloid Interface Sci.* **2007**, *305*, 62–71.
(5) Perrino, C.; Lee, S.; Choi, S. W.; Maruyama, A.; Spencer, N. D. *Langmuir* **2008**, *24*, 8850–8856.
(6) Pasche, S.; De Paul, S. M.; Vörös, J.; Spence, N. D.; Textor, M. *Langmuir* **2003**, *19*, 9216–9225.
(7) Naderi, A.; Iruthayaraj, J.; Vareikis, A.; Makuska, R.; Claesson, P. M. *Langmuir* **2007**, *23*, 12222–12232.
(8) Dedinaite, A.; Joseph, I.; Gorochovceva, N.; Makuska, R.; Claesson, P. M. *Prog. Colloid Polym. Sci.* **2006**, *132*, 124–130.
(9) Kenausis, L. G.; Voros, J.; Elbert, D.; Huang, N.; Hofer, R.; Ruiz-Taylor, L.; Textor, M.; Hubbell, J. A.; Spencer, N. D. *J. Phys. Chem. B* **2000**, *104*, 3298.
(10) Naderi, A.; Pettersson, T.; Makuska, R.; Claesson, P. M. *Langmuir* **2008**, *24*, 3336–3347.
(11) Pettersson, T.; Dedinaite, A. *J. Colloid Interface Sci.* **2008**, *324*, 246–256.

(12) Naderi, A.; Makuska, R.; Claesson, P. M. *J. Colloid Interface Sci.* **2008**, *323*, 191–202.
(13) Naderi, A.; Iruthayaraj, J.; Pettersson, T.; Makuska, R.; Claesson, P. M. *Langmuir* **2008**, *24*, 6676–6682.
(14) Naderi, A.; Olanya, G.; Makuska, R.; Claesson, P. M. *J. Colloid Interface Sci.* **2008**, *323*, 223–228.
(15) Olanya, G.; Iruthayaraj, J.; Poptoshev, E.; Makuska, R.; Vareikis, A.; Claesson, P. M. *Langmuir* **2008**, *24*, 5341–5349.
(16) Iruthayaraj, J.; Poptoshev, E.; Vareikis, A.; Makuska, R.; van der Wal, A.; Claesson, P. M. *Macromolecules* **2005**, *38*, 6152–6160.
(17) Iruthayaraj, J.; Olanya, G.; Claesson, P. M. *J. Phys Chem. C* **2008**, *112*, 15028–15036.
(18) Scheutjens, J. M. H. M.; Fleer, G. J. *J. Phys. Chem.* **1979**, *83*, 1619.
(19) Fleer, G. J.; Cohen Stuart, M. A.; Scheutjens, J. M. H. M.; Cosgrove, T.; Vincent, B. *Polymers at Interfaces*; Chapman & Hall: London, 1993.
(20) Linse, P. *Macromolecules* **1996**, *29*, 326–336.
(21) Leermakers, F. A. M.; Scheutjens, J. M. H. M. *J. Phys. Chem.* **1988**, *89*, 3264.
(22) Flory, P. J. *Principles of Polymer Chemistry*; Cornell University Press: Ithaca, NY, 1953.
(23) Karlström, G. *J. Phys. Chem.* **1985**, *89*, 4962–4964.
(24) Schillén, K.; Claesson, P. M.; Malmsten, M.; Linse, P.; Booth, C. *J. Phys. Chem.* **1997**, *101*, 4238–4252.
(25) Rubio, J.; Kitchener, J. A. *J. Colloid Interface Sci.* **1976**, *57*, 132.
(26) Eremenko, B. V.; Sergienko, Z. A. *Colloid J. USSR* **1979**, *41*, 353.
(27) Zhuravlev, L. T. *Langmuir* **1987**, *3*, 316.
(28) Rojas, O.; Ernstsson, M.; Neuman, R. D.; Claesson, P. M. *J. Phys. Chem. B* **2000**, *104*, 10032–10042.
(29) Wang, T. K.; Audebert, R. *J. Colloid Interface Sci.* **1988**, *121*, 32–41.
(30) Durand-Piana, G.; Lafuma, F.; Audebert, R. *J. Colloid Interface Sci.* **1987**, *119*, 474–480.
(31) Dedinaite, A.; Bastardo, L.; Oliveira, C. P.; Pedersen, J. S.; Claesson, P. M.; Vareikis, A.; Makuska, R. In *Proceedings of Baltic Polymer Symposium*; Makuska, R., Romaskevic, T., Ed.; Vinius University: Druskininkai, Lithuania, 2007, pp 112−116.
(32) Postmus, B. R.; Leermakers, F. A. M.; Cohen Stuart, M. A. *Langmuir* **2008**, *24*, 1930–1942.